Heliyon 9 (2023) e17279

Contents lists available at ScienceDirect

Heliyon

journal homepage: www.cell.com/heliyon

# A novel rabbit model of abdominal aortic aneurysm: Construction and evaluation

Changtao Qiu [a,b,1], Yuejin Li [b,1], Le Xiao [b], Jian Zhang [b], Shikui Guo [b], Peng Zhang [b], Ruoxi Li [b], Kunmei Gong [b,*]

[a] Affiliated Hospital of Kunming University of Science and Technology, Kunming, 650500, Yunnan, China
[b] Department of General Surgery, The First People's Hospital of Yunnan Province Kunming, Kunming, 650032, Yunnan, China

ARTICLE INFO

*Keywords:*
Abdominal aortic aneurysm
Animal model
Porcine pancreatic elastase
Balloon dilation

ABSTRACT

Prior research has indicated that animal models of abdominal aortic aneurysm (AAA) utilizing porcine pancreatic elastase (PPE) exhibit a perfusion duration of 30 min, and extended perfusion durations are associated with elevated mortality rates. Similarly, the AAA model, which relies solely on balloon dilation (BD), is limited by the occurrence of self-healing aneurysms. Consequently, we constructed a novel AAA model by PPE combined with balloon expansion to shorten the modeling time and improve the modeling success rate. The findings indicated that 5 min was the optimal BD time for rabbits, 3 min BD was ineffective for aneurysm formation, and 10 min BD had a high mortality rate. The model, constructed in combination with PPE and 5 min BD, exhibited a 100% model formation rate and a 244.7% ± 9.83% dilation rate. HE staining exhibited that severe disruption of the inner, middle, and outer membranes of the abdominal aorta, with a marked decrease in smooth muscle cells and elastase, and a marked increase in fibroblasts of the middle membrane, and many infiltrating inflammatory cells were seen in all three layers, especially in the middle membrane. EVG staining displayed that the elastic fibers of the abdominal aortic wall were fractured and degraded, and lost their normal wavy appearance. The protein expression of inflammatory factor (IL-1β, IL-6 and TNF-α) as well as extracellular matrix components (MMP-2 and MMP-9) were significantly increased compared to PPE and 5 min BD alone. In conclusion, PPE combined with BD allows the establishment of a novel AAA model that closely mimics human AAA in terms of histomorphology, inflammatory cell infiltration, and vascular stromal destruction. This model provides an ideal animal model for understanding the pathogenesis of AAA.

## 1. Introduction

Abdominal aortic aneurysm (AAA) is degenerative vascular disease with high risk in vascular surgery, which is characterized by progressive local dilatation of the abdominal aorta [1]. AAA incidence is as high as 12.5% among older men aged 75–84 years in the United States [2]. Once AAA ruptures, the overall mortality rate ranges from 65% to 85%, making it a life-threatening condition [3,4].

* Corresponding author. Department of General Surgery, the First People's Hospital of Yunnan Province, Affiliated Hospital of Kunming University of Science and Technology, No. 157 Jinbi Road, Kunming, 650032, Yunnan, China.
*E-mail address:* kunhuagongkunmei@163.com (K. Gong).
[1] Changtao Qiu and Yuejin Li contributed equally to this work.

https://doi.org/10.1016/j.heliyon.2023.e17279
Received 9 March 2023; Received in revised form 11 June 2023; Accepted 13 June 2023
Available online 14 June 2023

Currently, it is widely accepted that AAA is associated with family genetics, inflammatory response, extracellular matrix (ECM) remodeling and other factors involving immunology, molecular biology and genomics. The insidious nature of AAA pathogenesis, combined with the widespread availability of endovascular aneurysm repair (EVAR) and the low autopsy rate of 0.04%–0.07%, has made it increasingly challenging to obtain human AAA specimens [5]. Accordingly, it is essential to establish animal models to explore AAA pathogenesis, disease progression and evaluation of relevant therapeutic strategies [6].

Currently, small animal AAA models include chemical models induced by angiotensin II (Ang II), porcine pancreatic elastase (PPE), calcium chloride and β-aminopropionitrile, physical models induced by balloon dilation (BD), as well as genetic models [7,8]. The Ang II infused ApoE −/− mouse model is the most classical method for inducing AAA formation in mice. Nevertheless, in this model, the aneurysm is mostly located in the aorta or ascending aorta above the renal artery branches, which is inconsistent with the human one being mostly below the aortic valve [9]. Moreover, the consumables utilized in this model for experimentation are expensive. The pathological changes of AAA model constructed using PPE are more similar to those of human AAA, which better mimics the features of inflammatory cell infiltration, endogenous protease activation, ECM degradation, smooth muscle cell apoptosis, and thrombosis, representing an ideal modeling approach with a high rate of aneurysm formation [10,11]. Nevertheless, the disadvantages of this model include a high variability in the rate of aortic dilatation and an increased rupture risk due to degradation of many elastic and collagen fibers with increasing perfusion time, resulting in a high mortality. Furthermore, the model established by BD alone is similar to human AAA pathology, but suffers from the defect of self-healing aneurysms [12,13].

Therefore, we envisioned to reduce the arterial perfusion time for PPE, and combine it with BD to establish the animal model. This study is the first to apply PPE combined with BD in small animals and to refine the limitations and deficiencies associated with a single modeling method. It holds promise for constructing a stable and reliable AAA model with a high survival rate, high rate of aneurysm formation and satisfactory reproducibility.

## 2. Material and method

### 2.1. Animal and ethics statement

Sixty healthy New Zealand rabbits were purchased from the Experimental Animal Center of Kunming Medical University (Kunming, China). Male rabbits weighing 2500–3000 g and aged 3 months were used. The experiments involving animals were approved by the Animal Care and Use Ethics Committee of Kunming Medical University (Approval number: Kmmu20211597) and conformed to the Guide for the Care and Use of Laboratory Animals.

### 2.2. Grouping information

Sixty male rabbits were selected and randomly divided into the following groups: control group, balloon dilation (BD) group (divided into BD 3 min group, 5 min group, and 10 min group), porcine pancreatic elastase group (PPE) and porcine pancreatic elastase + Balloon dilation group (PPE + BD). There were 10 rabbits in each group.

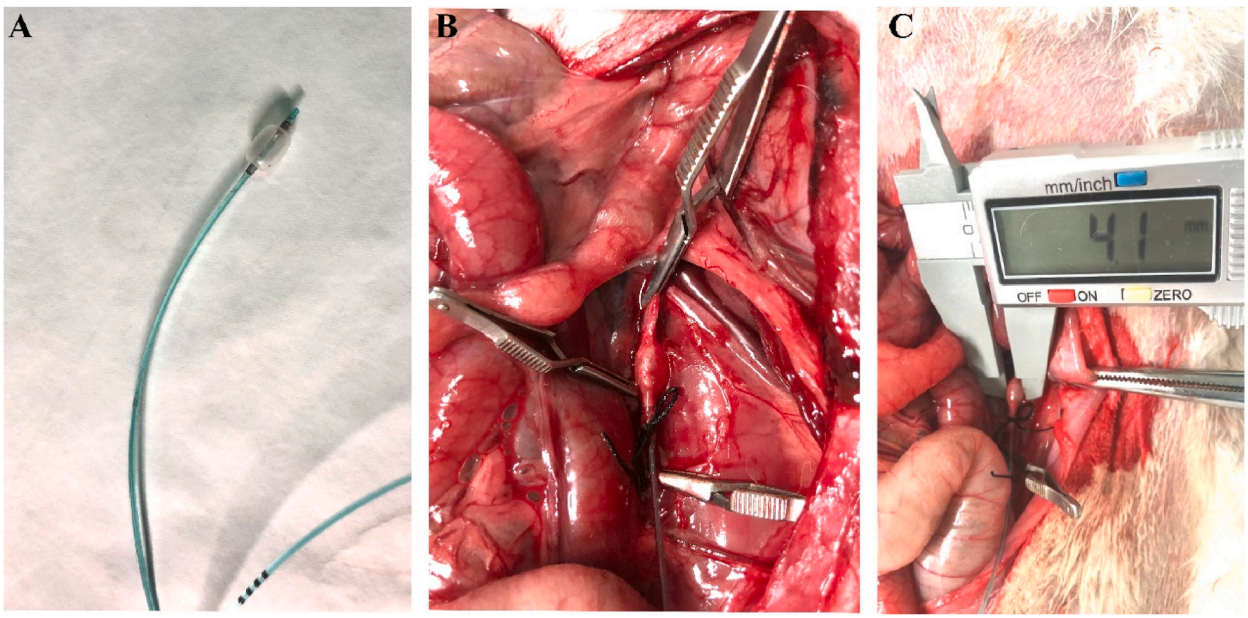


**Fig. 1.** The experimental procedure of the balloon dilatation-induced AAA model. A: 3F balloons under working pressure. B: Abdominal aorta was expanded up 1.5 times by 3F balloon. C: The dilated abdominal aorta was measured using a digital caliper.

### 2.3. BD model process

The experimental procedure for the BD-induced AAA model is shown in Fig. 1A–C. Heparin sodium (3000 U/kg) was injected intravenously and 3% sodium pentobarbital was used to anesthetize the rabbits. The rabbits were shaved and disinfected with iodophor. The rabbit was placed with supine position on the surgical area. A 10 cm incision was made in the middle of the abdomen to fully expose the infrarenal segment of the abdominal aorta. The tissue surrounding the abdominal aorta was separated with blunt dissection. Then, the abdominal aorta and inferior vena cava were carefully separated. The diameter of the infrarenal abdominal aorta was measured using vernier calipers and recorded. All branches of the aorta at the bifurcation of the intrarenal artery were closed using 9-0 sutures. The proximal and distal infrarenal abdominal aorta were blocked successively with blocking agents, and the distance between the two vascular clamps should be greater than 2 cm. A 2–3 mm incision was created 5 mm above the distal abdominal aortic block. A 3F balloon was inserted under working pressure, and then the abdominal aorta was directly dilated 1.5 times using syringe inflation for 3, 5, and 10 min, respectively. After the operation, the syringe was pumped back so that the balloon was completely free of pressure. The aortic stoma was closed with 9-0 sutures. The distal blocker was withdrawn first to observe any bleeding. Upon confirming no bleeding, the proximal blocker was slowly withdrawn. The blood flow in the abdominal aorta was restored, and the aortic stoma was checked for any bleeding. The instruments were counted, the abdomen was closed layer by layer. Penicillin was administered to rabbits postoperatively to prevent wound infection.

### 2.4. PPE model process

The experimental procedure for inducing AAA with PPE is illustrated in Fig. 2A and B. The anesthesia, dissociation of the abdominal aorta, and measurement procedures were the same as in the BD group. All aortic branches bifurcating between the renal arteries were ligated with 9-0 sutures. A 6-0 wire was placed in advance to ligate the proximal and distal portions around the aorta. This step is designed to prevent bleeding and failure of PPE to close the perfusion due to incomplete blockage of the vascular block. Then, an incision was made 5 mm above the distal ligature of the abdominal aorta. During this period, if there is a PPE leak, the 6-0 wire should be tightened in time to ensure the normal infusion of PPE. A 30U PPE was perfused with an airtight PE-10 catheter for 30 min. During this period, if PPE leaks, it is replenished promptly so that the abdominal aorta is always fully supplied. After the procedure, the drug was withdrawn and flushed with saline. The vessel was closed using 10-0 silk sutures. Wound closure and postoperative care were performed according to the process described in the BD model.

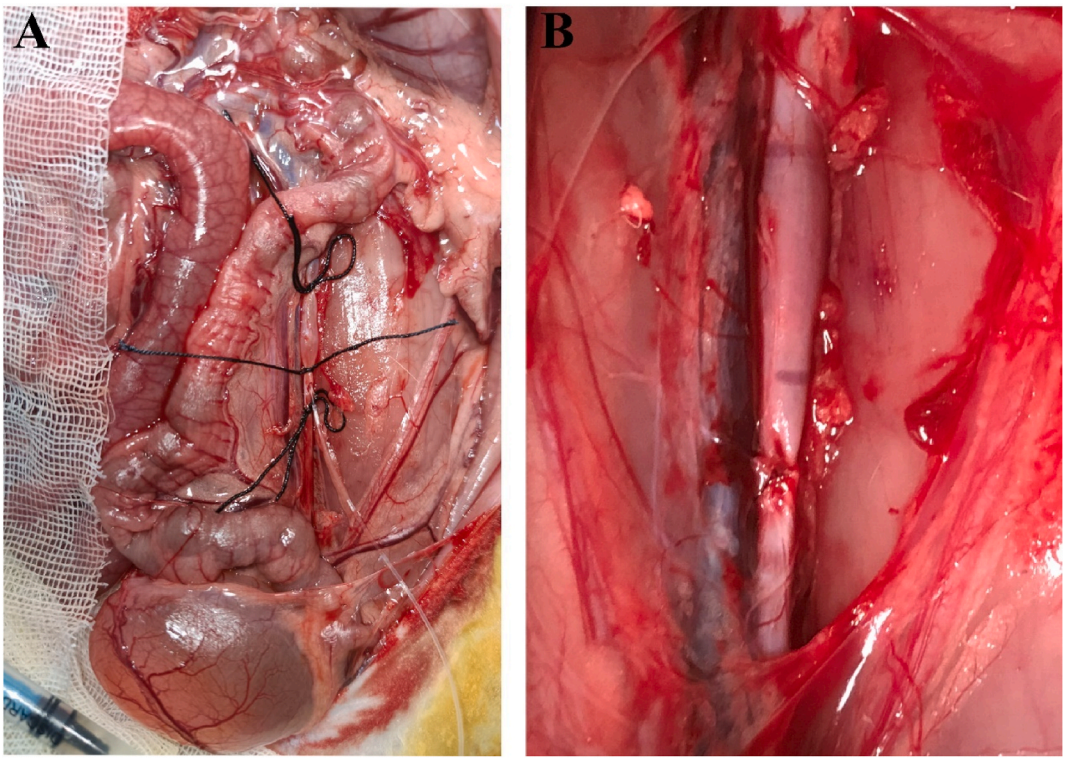


**Fig. 2.** The experimental procedure of the porcine pancreatic elastase-induced AAA model. A: porcine pancreatic elastase was injected into the lower abdominal aorta of the kidney. B: Postoperative morphological changes of abdominal aortic segment.

### 2.5. PPE + BD model process

The flowchart of PPE combined with BD to construct the AAA model is displayed in Fig. 3. In short, the balloon was dilated for 5 min based on combined PPE perfusion for 15 min, and the procedure was the same as balloon dilatation and PPE infusion.

### 2.6. Calculation of the expansion rate and formation rate of AAA diameter

Aneurysm expansion rate = abdominal aortic diameter at 4 weeks after preoperative diameter/abdominal aortic diameter at preoperative × 100%. Aneurysm formation rate = abdominal aortic diameter at 4 weeks after preoperative diameter >50%, which is considered as the formation of AAA.

### 2.7. Specimen collection and processing

Postoperative feeding was routine, euthanasia was performed after 28 d, and abdominal aortic tissue was collected for follow-up experiments. The abdominal aortic tissue was cut and immersed in saline solution to remove any remaining blood. Then, the abdominal aortic tissue was fixed in 4% paraformaldehyde for 12 h and embedded in paraffin.

### 2.8. Histopathological analysis

Hematoxylin-eosin (HE) Staining and Verhoeff-van Gieson (EVG) staining were carried out for histopathological analysis of the abdominal aorta in each group. Slices of 4 μm thickness were prepared using a slicer (RM2235, Leica). Slices were dewaxed using xylene and ethanol, drained and set aside. HE staining and EVG staining were performed by Hematoxylin-Eosin (HE) Stain Kit (Solarbio, China) and Verhöeff Elastic Fiber Staining Kit (Solarbio), respectively. For HE staining, sections were first stained using hematoxylin for 15 min and then eosin was used to continue staining for 5 min. For EVG staining, sections were stained with Verhöeff staining solution for 20 min and differentiated with Verhöeff differentiation solution for 10–20 s. After being treatment with 95% anhydrous ethanol for 4 min, the sections were re-stained with eosin for 1 min. The stained HE and EVG sections were dehydrated and transparent using anhydrous ethanol and xylene, respectively. After sealing, HE and EVG-stained sections were scanned using a Pannoramic MIDI scanner (3DHISTECH, HU).

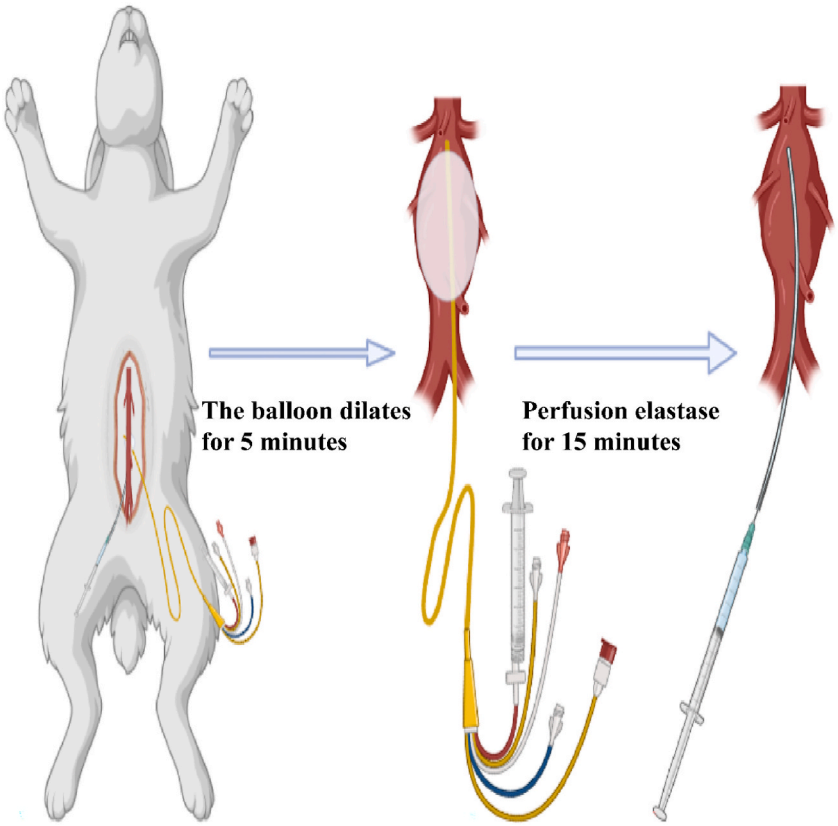


**Fig. 3.** Schematic diagram of AAA was established by porcine pancreatic elastase combined with balloon dilation.

### 2.9. Immunohistochemical staining

Immunohistochemical (IHC) staining was used to analyze the proportion of matrix metalloproteinase-2 (MMP-2) and matrix metalloproteinase-2 (MMP-9) positive cells in the abdominal aortic tissue of each group. Sections were prepared and dewaxed as described in the Histopathological analysis procedure. Then, the tissue sections were incubated with 1% $H_2O_2$ in methanol for 20 min to block endogenous peroxidase activity. Non-specific binding was blocked with 5% goat serum at room temperature for 30 min. MMP-2 rabbit monoclonal antibody (bs-4599R; 1: 450; Bioss, China) and MMP-9 mouse monoclonal antibody (ab58803; 1: 300; Abcam, UK) were dropped in tissue sections and incubated overnight in a refrigerator at 4 °C. After washing with PBS, Enhanced enzyme-labeled goat anti-mouse/Rabbit IgG polymer (PV-9000; ZSGB-BIO, China) was dropped in tissue sections and incubated for 20 min. After color development with DAB color development kit (ZL1-9019; ZSGB-BIO), the sections were re-stained for 5 min using hematoxylin staining solution. After sealing, IHC-stained sections were scanned using a Pannoramic MIDI scanner.

### 2.10. Western blotting assay

Tissue homogenates were prepared from abdominal aortic aneurysm tissue, and total protein was extracted using RIPA lysis buffer (Beyotime, China). After using the BCA Protein Assay Kit (Beyotime) to quantify total proteins, the expression of the target proteins was measured using primary antibodies to MMP-2 (1: 1000), MMP-9 (1: 2000), Interleukin-1β (IL-1β; bs-0812R; 1: 1000; bioss, China), Interleukin-6 (IL-6; MBS2106142; 1: 1000; MyBioSource, USA), Tumor Necrosis Factor-α (TNF-α; MBS2038526; 1: 1000; MyBioSource, USA), and β-actin (TA-09; 1: 2000; ZS-Bio). Secondary antibody was Enhanced enzyme-labeled goat anti-mouse/Rabbit IgG polymer. The membranes were developed using an ECL kit (Beyotime). The membranes were imaged and photographed using a 5200-multi gel imaging system (Tanon, China). The density of grayscale values was analyzed with Image J software. β-actin was used as an internal reference.

### 2.11. Statistical methods

The chi-square test or Fisher's exact probability method was performed using GraphPad Prism 8.0. The Mann-Whitney test was utilized for comparing measurement data between two groups, and the Kruskal-Wallis H test was used to compare measurement data among multiple groups. If $P < 0.05$, the difference was statistically significant. Image analysis was performed using Image J and Image-Pro Plus 6.0 software.

## 3. Results

### 3.1. Rabbit survival rate, expansion rate and AAA formation rate

The survival rate in the PPE + BD group was 80%. Their deaths were primarily caused by spinal cord ischemia, postoperative thrombosis, and rupture of the separated aorta and inferior vena cava. The expansion rate was 244.7% ± 9.83%. The aneurysm rate was 100%. The survival rate, expansion rate and aneurysm rate of all groups are shown in Table 1 and Fig. 4A–D.

### 3.2. Histopathological morphology of each model

The results of HE staining are shown in Fig. 5A. The Control group displayed no significant thickening of the arterial wall, the three layers of the inner and outer membranes were intact, the elastic fibers were wavy, continuous and uniform, without loss or fracture, smooth muscle cells were clearly visible and uniformly distributed, and no inflammatory cell infiltration was seen. The structure of the arterial wall was slightly disturbed, and the elastic fibers were slightly degraded, but the structure of each layer was still clear in the BD 3 min, BD 5 min and BD 10 min groups. In the PPE and PPE + BD groups, the arterial wall had an irregular structure, partial thickening of the outer membrane, unclear structure of the layers, disorganized morphology of smooth muscle cells, and infiltration of inflammatory cells.

The results of EVG staining are shown in Fig. 5B. In the Control group, the abdominal aortic wall was neatly structured and the elastic fibers were evenly arranged, the elastic fibers were reduced in a small amount and the collagen fibers were relatively increased in the BD 3 min, BD 5 min and BD 10 min groups. The PPE and the PPE + Balloon groups had degeneration and atrophy of the smooth

**Table 1**
Outcome of survival rate, AAA rate expansion rate and diameter expansion rate in each group.

| Groups | Technique Success Rate (%) | Survival Rate (%) | AAA Incidence (%) | Diameter Expansion Rate (%) |
|---|---|---|---|---|
| Control | 10 (100) | 10 (100) | 0 (0) | 110.6±4.33 |
| BD 3min | 10 (100) | 10 (100) | 0 (0) | 142.8±6.56 |
| BD 5min | 10 (100) | 10 (100) | 2 (20) | 149.7±5.74 |
| BD 10min | 10 (100) | 6 (60) | 2 (33.33) | 150.3±9.64 |
| PPE | 10 (100) | 8 (80) | 6 (75) | 174.6±23.2 |
| PPE + BD | 10 (100) | 8 (80) | 8 (100) | 244.7±9.83 |

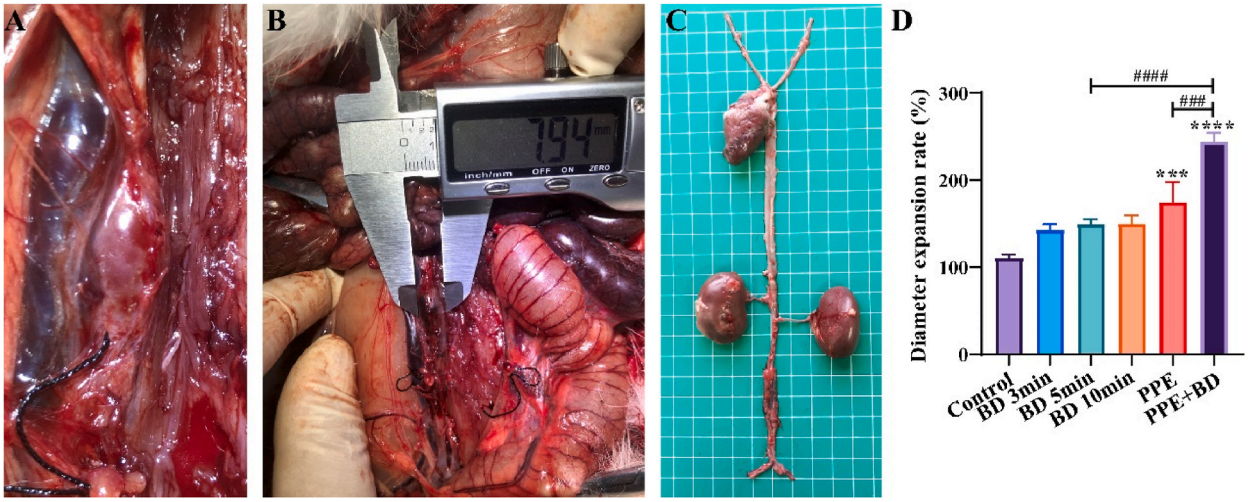


**Fig. 4.** Expansion rate of each model. A: The shape of AAA in PPE + BD group showed fusiform, and the aneurysm formation effect was satisfactory. B: Representative images of the measurement in abdominal aortic diameter. C: Representative images of the abdominal aorta in the PPE + BD group. D: Comparison of the expansion rate of each model group. Compared to the Control group, $^{***}P < 0.001$, $^{****}P < 0.0001$.

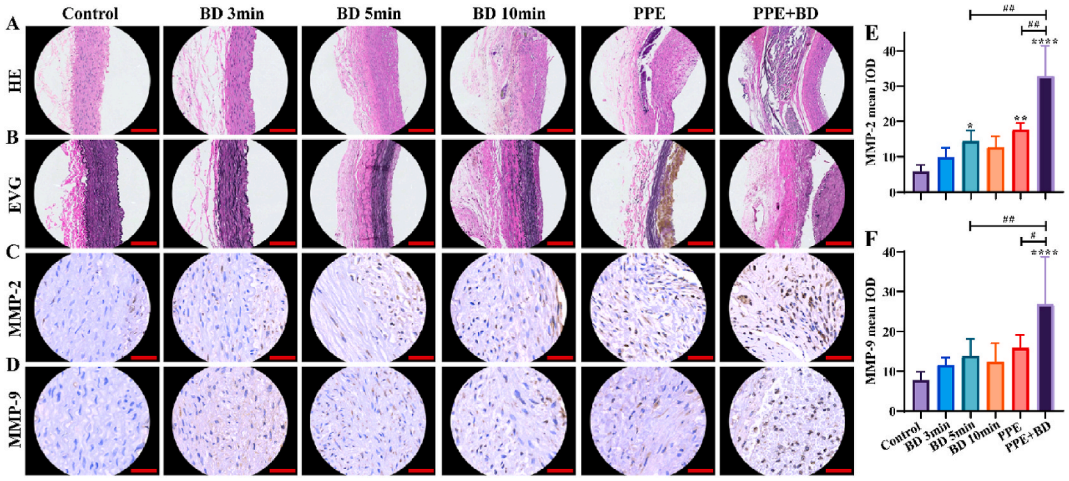


**Fig. 5.** Histopathological morphology of each model. A. Representative pictures of HE staining in different groups. B. Representative images of EVG staining in different group. C-D. Representative pictures of IHC staining for (C) MMP-2 and (D) MMP-9 in different group. E–F: Statistical analysis of (E) MMP-2 and (F) MMP-9 positive area in the abdominal aortic tissue of each model. Scale bar: 50 μm. Magnification: 40×. Compared to the Control group, $^{*}P < 0.05$, $^{**}P < 0.01$, $^{****}P < 0.0001$.

muscle cells in the middle layer of the vessel, and the elastic fibers were significantly reduced and the amount of collagen fibers was increased in a large amount.

It is suggested that the pathological changes in the AAA model constructed by PPE combined with BD are more marked and more similar to human AAA than those using PPE or BD alone.

### 3.3. Evaluation of ECM degradation in the abdominal aorta tissue

To understand the ECM remodeling in each model, we examined the percentage of positive MMP-2 and MMP-9 in abdominal aortic tissue using IHC. The results of IHC staining for MMP-2 and MMP-9 are shown in Fig. 5C–F. The positive area for MMP-2 was significantly higher in the BD 5min and PEE groups than in the Control group ($P < 0.05$). There was no significant difference in the positive area of MMP-9 in the Control, BD 3 min, BD 5 min, BD 10 min and PPE groups ($P > 0.05$). Notably, the positive area for both MMP-2 and MMP-9 was significantly greater in the PPE + BD group than in the Control group ($P < 0.05$). Likewise, their expression was significantly increased compared to BD 5min and PPE groups. It is indicated that the ECM degradation of the AAA model constructed by PPE combined with BD is more severe.

### 3.4. Evaluation of inflammation in the abdominal aorta tissue

To explore the inflammatory profile of each model, we measured the levels of pro-inflammatory factors IL-1β, IL-6 and TNF-α protein in abdominal aortic tissue. Compared with the Control group, the levels of IL-1β, IL-6 and TNF-α proteins were significantly elevated in each model group (Fig. 6A–D, $P < 0.05$). Interestingly, the expression of IL-1β, IL-6 and TNF-α proteins was significantly stronger in the AAA model constructed with PPE combined with BD than with PPE or BD alone (Fig. 6A–D, $P < 0.05$). It is worth noting that the expression of MMP-9 protein in the PPE + BD group was significantly increased than that in the BD 5 min and PPE groups (Fig. 6E–F, $P < 0.05$), which is consistent with the IHC staining results. It is indicated that the inflammation in the AAA model constructed by PPE combined with BD is heavier than that of PPE or BD alone.

## 4. Discussion

The pathogenesis of AAA is still unclear, and appropriate animal models of AAA are crucial for studying disease's pathogenesis, diagnosis, and treatment. Currently, animal models for AAA are being constructed and developed rapidly, with chemical methods being the mainstream and practical approach. It provides a practical basis for studying the pathogenesis and treatment of AAA. The principle of aneurysm formation is that PPE lyses the perfused tissue of the abdominal aorta, initiating the inflammatory and apoptotic program of smooth muscle in the abdominal aorta, resulting in the disruption of the balance of arterial wall elastin and collagen self-renewal, which eventually leads to the inability of the abdominal aortic wall to resist arterial pressure and dilates outward, forming an AAA [14]. Animal models of AAA can be classified into three categories: physical, chemical, and genetic induction manners [10,15]. Anidjar et al. [16] first reported the establishment of animal models in rats by intraluminal pressurized perfusion of PPE for 2 h. The literature reports perfusion times ranging from 3 to 30 min [17–19]. This method has since been modeled by scholars and is one of the most commonly used chemical model, and a large number of reports have demonstrated the feasibility of this method [20–22].

There are few reports on the establishment of physical injury animal models using BD, and our experience suggests that BD causes endothelial damage, allowing for easier PPE perfusion entry into the aortic mesentery. This may result in shorter aneurysm formation time, better aneurysm formation, and more pronounced aneurysms. Previous articles have reported that BD combined with chemical induction are applied to large animal models. Robert et al. [23] constructed a porcine infrarenal AAA model using a combination of PPE and collagenase, along with BD. They used a 12 mm diameter, 2 cm length vascular balloon and observed a 194% increase in aortic diameter compared to preoperative images acquired at 6 weeks. Alexander et al. [24] successfully constructed a porcine infrarenal AAA model using a 16 mm diameter balloon with a dilation time of 10 min, supplemented with oral β-aminopropionitrile, resulting in an AAA dilation rate of 113.5% ± 30.2% at 28 days postoperatively. However, the studies mentioned above were conducted on large animals, and there are no reports on the study of BD combined with chemical induction in small animal models. We shortened the time

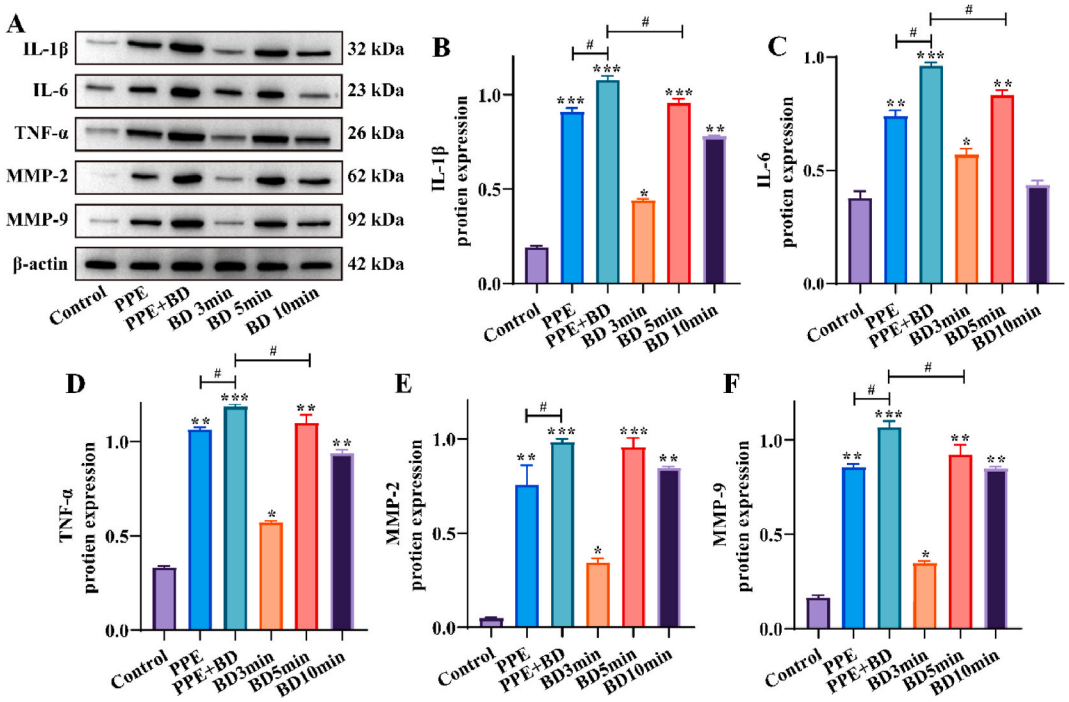


**Fig. 6.** Expression of inflammation- and ECM-related proteins in each model group. A: Representative images of IL-1, IL-6, TNF-α, MMP-2, MMP-9 and β-actin gels. The original gel blots can be obtained from the supplementary material. B–F: Statistical analysis of the expression of (B) IL-1, (C) IL-6, (D) TNF-α, (E) MMP-2, (F) MMP-9 in each model group. Compared to the Control group, $^{*}P < 0.05$, $^{**}P < 0.01$, $^{***}P < 0.001$, $^{****}P < 0.0001$.

of PPE perfusion from the conventional 30 min to 15 min. Additionally, we discovered that 5 min of balloon expansion is the most optimal time for balloon expansion in rabbits, 3 min of balloon expansion of aneurysm formation is not effective, and 10 min of balloon expansion has a relatively high mortality rate. We believe that spinal cord ischemia and postoperative thrombosis caused the death of four rabbits in the 10 min balloon group, following lower limb paralysis at 1 and 2 days postoperatively. Since, arterial thrombosis was seen in the collected abdominal aortic specimens. Classical PPE perfusion requires maintenance of 120 mmHg perfusion pressure using either hydraulic or micropump syringe. However, it can be challenging to accurately reach and maintain the same pressure. Excessive perfusion pressure not only causes PPE to easily enter the blood stream, leading to acute pancreatitis-induced tissue damage, but also PPE spills out into the lumen, causing damage to the entire lumen and surrounding tissues, which directly results in vascular rupture and hemorrhagic death of the animal [11,25,26]. In this study, it should be considered that 5 min of BD was also required in the PPE + BD group, and an additional 15 min of pressurized perfusion would certainly lead to increased mortality in rabbits. Therefore, we slowly injected PPE into the perfused portion of the abdominal aorta to keep it filled, and shortened the PPE perfusion time from the conventional 30 min–15 min, which resulted in less damage to the vessels. This method is simpler and more easily replicable.

This study confirmed the feasibility of constructing AAA model using PPE combined with BD. The aneurysm formation rate was 100%, and the aneurysm shape was fusiform, which is more compatible with the morphology of human AAA. MMP-2 and MMP-9 play the main role in AAA [27–29]. The results of this study also confirmed the elevated expression of inflammatory factors IL-1β, IL-6, TNF-α, as well as MMP-2 and MMP-9, which are consistent with the pathological changes of AAA. The expression of MMP-2 and MMP-9 in PPE + BD group was significantly higher than that in PPE group. Under the same survival rate, the effect of aneurysm formation rate was better in PPE + BD group than that in PPE group.

The report has some limitations. Due to economic reasons, the changes of abdominal aorta were not dynamically observed by color ultrasound following induction of AAA. Color Doppler ultrasound helps monitor the timing of aneurysm formation.

In conclusion, this model reduced the mortality of experimental animals and increased the rate of aneurysm formation by reducing the perfusion time of PPE combined with BD. The study demonstrated that 5 min of BD is the appropriate dilation time for rabbits to form aneurysms, 3 min of BD is not effective, and 10 min of BD has relatively high mortality rate. In addition, this model was similar to human AAA in histomorphology, inflammatory cell infiltration and vascular matrix destruction. Therefore, PPE combined with BD has the characteristics of stability, reliability, high survival rate, high aneurysm formation rate and satisfactory reproducibility. It is an ideal animal model to study the pathogenesis of AAA.

## Declaration

### *Ethics approval*

The experiments involving animals were approved by the Animal Care and Use Ethics Committee of Kunming Medical University (Approval number: Kmmu20211597).

### *Consent for publication*

Not applicable.

### *Availability of data and materials*

All the data obtained and materials analyzed in this research are available with the corresponding author upon reasonable request.

### *Funding*

This work was supported by the National Natural Science Foundation of China (81960447), and the Chen Zhong Expert Workstation Fund of Yunnan Province (2005AF150018).

### *Authors' contributions*

C.Q. performed experiments, analyzed and interpreted the data, and wrote the paper;
Y.L. conceived and designed the experiments, and wrote the paper;
L.X. performed the experiments;
J.Z. performed the experiments;
S.G. performed the experiments;
P.Z. performed the experiments;
R.L. analyzed and interpreted the data;
K.G. conceived and designed the experiments, contributed reagents, materials, analysis tools or data, and wrote the paper;
All the authors read and approved the final draft.

## Declaration of competing interest

The authors declare that they have no known competing financial interests or personal relationships that could have appeared to influence the work reported in this paper

## Acknowledgements

Not applicable.

## References

[1] K. Haque, P. Bhargava, Abdominal aortic aneurysm, Am. Fam. Physician 106 (2) (2022) 165–172.
[2] E.J. Benjamin, et al., Heart disease and stroke statistics-2019 update: a report from the American Heart Association, Circulation 139 (10) (2019) e56–e528.
[3] N. Sakalihasan, et al., Abdominal aortic aneurysms, Nat. Rev. Dis. Prim. 4 (1) (2018) 34.
[4] B.T. Baxter, M.C. Terrin, R.L. Dalman, Medical management of small abdominal aortic aneurysms, Circulation 117 (14) (2008) 1883–1889.
[5] J.C. Tsui, Experimental models of abdominal aortic aneurysms, Open Cardiovasc. Med. J. 4 (2010) 221–230.
[6] M. Thompson, G. Cockerill, Matrix metalloproteinase-2: the forgotten enzyme in aneurysm pathogenesis, Ann. N. Y. Acad. Sci. 1085 (2006) 170–174.
[7] J. Golledge, S.M. Krishna, Y. Wang, Mouse models for abdominal aortic aneurysm, Br. J. Pharmacol. 179 (5) (2022) 792–810.
[8] H. Tanaka, et al., The role of animal models in elucidating the etiology and pathology of abdominal aortic aneurysms: development of a novel rupture mechanism model, Ann. Vasc. Surg. 63 (2020) 382–390.
[9] B. Trachet, et al., Angiotensin II infusion into ApoE-/- mice: a model for aortic dissection rather than abdominal aortic aneurysm? Cardiovasc. Res. 113 (10) (2017) 1230–1242.
[10] J. Golledge, Abdominal aortic aneurysm: update on pathogenesis and medical treatments, Nat. Rev. Cardiol. 16 (4) (2019) 225–242.
[11] Y. Bi, et al., Performance of a modified rabbit model of abdominal aortic aneurysm induced by topical application of porcine elastase: 5-month follow-up study, Eur. J. Vasc. Endovasc. Surg. 45 (2) (2013) 145–152.
[12] M.J. Hallisey, SCVIR Gary J. Becker Young Investigator Award paper. A transluminally created abdominal aortic aneurysm model, J. Vasc. Intervent. Radiol. 8 (3) (1997) 305–312.
[13] A. Czerski, et al., Experimental methods of abdominal aortic aneurysm creation in swine as a large animal model, J. Physiol. Pharmacol. 64 (2) (2013) 185–192.
[14] N. Patelis, et al., Animal models in the research of abdominal aortic aneurysms development, Physiol. Res. 66 (6) (2017) 899–915.
[15] J. Silence, D. Collen, H.R. Lijnen, Reduced atherosclerotic plaque but enhanced aneurysm formation in mice with inactivation of the tissue inhibitor of metalloproteinase-1 (TIMP-1) gene, Circ. Res. 90 (8) (2002) 897–903.
[16] S. Anidjar, et al., Elastase-induced experimental aneurysms in rats, Circulation 82 (3) (1990) 973–981.
[17] A.C. Chiou, et al., Transrectal ultrasound assessment of murine aorta and iliac arteries, J. Surg. Res. 88 (2) (2000) 193–199.
[18] G.G. Deng, et al., Urokinase-type plasminogen activator plays a critical role in angiotensin II-induced abdominal aortic aneurysm, Circ. Res. 92 (5) (2003) 510–517.
[19] C. Barisione, et al., Rapid dilation of the abdominal aorta during infusion of angiotensin II detected by noninvasive high-frequency ultrasonography, J. Vasc. Surg. 44 (2) (2006) 372–376.
[20] C.M. Bhamidipati, et al., Development of a novel murine model of aortic aneurysms using peri-adventitial elastase, Surgery 152 (2) (2012) 238–246.
[21] T.M. Joergensen, et al., Abdominal aortic diameter is increased in males with a family history of abdominal aortic aneurysms: results from the Danish VIVA-trial, Eur. J. Vasc. Endovasc. Surg. 48 (6) (2014) 669–675.
[22] H. Kurvers, et al., Discontinuous, staccato growth of abdominal aortic aneurysms, J. Am. Coll. Surg. 199 (5) (2004) 709–715.
[23] R.L. Hynecek, et al., The creation of an infrarenal aneurysm within the native abdominal aorta of swine, Surgery 142 (2) (2007) 143–149.
[24] A.H. Shannon, et al., Porcine model of infrarenal abdominal aortic aneurysm, J. Vis. Exp. (153) (2019).
[25] J.X. Zhu, et al., Establishment of a New abdominal aortic aneurysm model in rats by a retroperitoneal approach, Front. Cardiovasc. Med. 9 (2022), 808732.
[26] Q. Zhang, et al., Suppression of experimental abdominal aortic aneurysm in a rat model by the phosphodiesterase 3 inhibitor cilostazol, J. Surg. Res. 167 (2) (2011) e385–e393.
[27] K. Miyagawa, et al., Loss of MURC/Cavin-4 induces JNK and MMP-9 activity enhancement in vascular smooth muscle cells and exacerbates abdominal aortic aneurysm, Biochem. Biophys. Res. Commun. 487 (3) (2017) 587–593.
[28] T. Li, et al., Matrix metalloproteinase family polymorphisms and the risk of aortic aneurysmal diseases: a systematic review and meta-analysis, Clin. Genet. 93 (1) (2018) 15–32.
[29] S. Paghdar, et al., Doxycycline therapy for abdominal aortic aneurysm: inhibitory effect on matrix metalloproteinases, Cureus 13 (5) (2021), e14966.